Exploring the Strong Interaction of Three-Body Systems at the LHC

S. Acharya *et al.*[*]
(ALICE Collaboration)

Deuterons are atomic nuclei composed of a neutron and a proton held together by the strong interaction. Unbound ensembles composed of a deuteron and a third nucleon have been investigated in the past using scattering experiments, and they constitute a fundamental reference in nuclear physics to constrain nuclear interactions and the properties of nuclei. In this work, K^+-d and p-d femtoscopic correlations measured by the ALICE Collaboration in proton-proton (pp) collisions at $\sqrt{s} = 13$ TeV at the Large Hadron Collider (LHC) are presented. It is demonstrated that correlations in momentum space between deuterons and kaons or protons allow us to study three-hadron systems at distances comparable with the proton radius. The analysis of the K^+-d correlation shows that the relative distances at which deuterons and protons or kaons are produced are around 2 fm. The analysis of the p-d correlation shows that only a full three-body calculation that accounts for the internal structure of the deuteron can explain the data. In particular, the sensitivity of the observable to the short-range part of the interaction is demonstrated. These results indicate that correlations involving light nuclei in pp collisions at the LHC will also provide access to any three-body system in the strange and charm sectors.

Subject Areas: Particles and Fields

I. INTRODUCTION

The study of multibody systems is a key aspect of modern nuclear physics because of its relevance for the structure of nuclear bound states [1–3] and for the equation of state of dense nuclear matter [4,5]. Effects that go beyond the simple addition of the strong interaction between pairs of nucleons emerge already in the description of the most basic properties of light nuclei. Realistic potentials describing nucleon-nucleon interactions [6,7] have therefore been complemented with phenomenological models of three-nucleon forces [8,9]. In calculations using potentials derived from chiral effective field theories (EFTs) [2,10], the multibody forces appear naturally as subleading terms in the chiral expansion. They find contributions of the order of 10% to the ground-state energies of $A \leq 12$ nuclei from genuine three-body nucleon forces [11,12], and deliver predictions for heavier and neutron-rich nuclear structures.

In this context, two-nucleon scattering data and properties of the $A = 3$ systems are still the most important ingredients to constrain the parameters of nuclear interactions derived from EFT [13–15]. In particular, differential

[*]Full author list given at the end of the article.

scattering observables for the p-d system have allowed for the computation of a full-fledged three-body wave function that accounts for all the relevant two- and three-body interactions at work in the p-(pn) system for the short and the asymptotic ranges, providing an excellent description of the p-d scattering data [16–18]. In this work, it is demonstrated that such a standard candle of the three-body nuclear interaction can also be investigated by means of p-d correlations in momentum space measured at the LHC.

Momentum correlations of the deuteron with other hadron species have already been considered as a tool to study both the deuteron production mechanism [19] and the final-state interactions for multibody systems. Different experimental correlations such as p-d and d-d have been measured [20–23] in O-Au reactions at $E/A = 25$, 35, and 60 MeV and in ^{40}Ar-^{58}Ni reactions at 77 MeV/u. The data showed a clear signature of the strong final-state interaction among light nuclei and nucleons, but the specific description of the process from a multibody perspective, as well as the tools to precisely measure the relative distances between particles, were not available at the time of those analyses.

Deuteron-hadron momentum correlations can also be investigated at the LHC, since light (anti)nuclei can be abundantly produced and accurately measured in ultrarelativistic nucleus-nucleus collisions [24–32]. Recent femtoscopy analyses carried out by ALICE in pp, p-Pb, and Pb-Pb collisions have demonstrated that it is possible to study the strong interaction among several hadron pairs [33–39] given the short distances at which hadrons can be produced in such colliding systems [40].

In this work, by means of a comprehensive study of the K^+-d and p-d correlation functions measured in pp collisions at center-of-mass energy $\sqrt{s} = 13$ TeV with the ALICE detector at the LHC, evidence is provided that deuterons are formed at average distances of the order of 2 fm from other hadrons. The measurement of the p-d correlation at such short distances constitutes an innovative method to study three-body systems at the LHC, with the potential of extending such studies to the strangeness and charm sectors. Indeed, in the strangeness sector, a similar approach to the one adopted for standard nuclear physics is envisaged for the future by improving the database of hypernuclei [41–43], scattering experiments [44], and femtoscopy measurements in hadron-hadron collisions [45,46]. Direct measurements of the hyperon-deuteron systems at short distances would provide complementary information to these standard methods.

II. CORRELATION FUNCTION FROM SCATTERING PARAMETERS

Final-state interactions involving light nuclei such as deuterons have been studied in the past via scattering experiments [47–51]. In scattering theory, the nuclear interaction in the asymptotic regime can be investigated by associating a plane wave with the incoming particle and building the outgoing wave as a superposition of spherical waves with phase shifts δ_l, with l denoting the relative angular momentum between the projectile and the target. The interaction determines the values of δ_l, and for $l = 0$, referred to as s-wave scattering, a scattering length a_0 is commonly used to characterize the interaction at zero energy and can be related to the differential cross section measured in scattering experiments. These measurements also enable the determination of the effective range of the interaction d_0.

Scattering experiments have been already performed for the K^+-d and p-d systems allowing for the extraction of the

corresponding scattering parameters, as reported in Table I. In the case of K^+-d, such parameters are spin averaged, and they are calculated with two different methods: (i) via an effective range fit (ER) to the cross-section predictions at threshold anchored to the available scattering data [52] and (ii) from the well-known K-N interactions [53] using the fixed-center approximation (FCA) [54]. The negative values of the K^+-d scattering length (a_0) refer to a repulsive strong interaction. In the case of the p-d system, the parameters for the spin doublet ($S = 1/2$) and quartet ($S = 3/2$) channels were obtained by using theoretical calculations [55–59] and a vast collection of scattering data [47–51]. The positive sign of the p-d scattering parameters reported in Table I corresponds to a repulsive interaction for the quartet state ($S = 3/2$), but for the doublet state ($S = 1/2$), the ^{3}He bound state emerges, and the standard effective range expansion has to be modified [see Eq. (2) in Ref. [58]].

An alternative method to test the accuracy of the relative wave function in a two-hadron system is the measurement of the correlation function among the pairs of interest produced in hadron-hadron collisions [36]. The theoretical correlation function can be expressed [60,61] as $C(k^*) = \int d^3 r^* S(r^*) |\psi(\mathbf{k}^*, \mathbf{r}^*)|^2$, where $S(r^*)$ is the distribution of the distance r^* between the emitted particles in a hadron-hadron collision defining the particle source, $\psi(\mathbf{k}^*, \mathbf{r}^*)$ represents the wave function of the relative motion for the pair of interest, and k^* is the reduced relative momentum of the pair ($k^* = |\mathbf{p}_2^* - \mathbf{p}_1^*|/2$). The asterisk indicates that the quantities are evaluated in the pair rest frame, where $\mathbf{p}_1^* = -\mathbf{p}_2^*$. The Lednický-Lyuboshitz (LL) formalism [62,63] provides a simplified analytical treatment of the wave function (see the Appendix for details) that can relate the correlation function to its asymptotic behavior where the core nuclear strong interaction is not considered. The analytical formula for the correlation function is obtained assuming a Gaussian source distribution in r^* and a single set of scattering

TABLE I. Scattering lengths a_0 and effective ranges d_0 for the p-d and K^+-d s-wave states. For the p-d, the two spin states (doublet and quartet) are reported. For the meson-baryon system, the negative values of scattering length refer to a repulsive interaction. For the baryon-baryon system, negative and positive values of a_0 refer to attractive and repulsive interactions (for cases where the potential does not support two-body bound states), respectively.

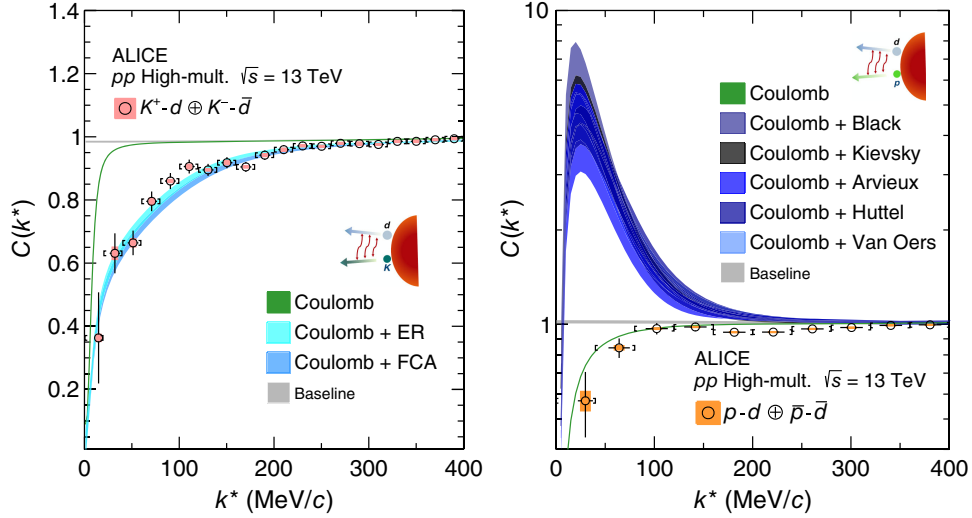| System | Spin averaged | | $S = 1/2$ | | $S = 3/2$ | | References |
	a_0 (fm)	d_0 (fm)	a_0 (fm)	d_0 (fm)	a_0 (fm)	d_0 (fm)	
K^+-d	-0.470	1.75	$\cdots$	$\cdots$	$\cdots$	$\cdots$	ER [52]
	-0.540	0.0	$\cdots$	$\cdots$	$\cdots$	$\cdots$	FCA [53,54]
p-d			$2.73^{+0.10}_{-0.10}$	$2.27^{+0.12}_{-0.12}$	$11.88^{-0.10}_{+0.40}$	$2.63^{+0.01}_{-0.02}$	Arvieux [55]
			$1.30^{+0.20}_{-0.20}$	$\cdots$	$11.40^{+1.80}_{-1.20}$	$2.05^{+0.25}_{-0.25}$	Van Oers [56]
			4.0	$\cdots$	11.1	$\cdots$	Huttel *et al.* [57]
			0.024	$\cdots$	13.8	$\cdots$	Kievsky *et al.* [58]
			$-0.13^{+0.04}_{-0.04}$	$\cdots$	$14.70^{+2.30}_{-2.30}$	$\cdots$	Black *et al.* [59]

FIG. 1.   Measured K^+-d (left) and p-d (right) correlation functions. The data are shown by the black symbols; the bars and the colored boxes represent the statistical and systematic uncertainties, respectively. The square brackets show the bin width of the measurement, while the horizontal black lines represent the statistical uncertainty in the determination of the mean k^* for each bin. Data are compared with theoretical correlation functions shown by colored bands obtained using the LL approximation. The bandwidths represent the uncertainties in the determination of the radius and the residual contributions. See text for details.

parameters. The formula is averaged over spin and isospin and considers only s wave in the scattering process.

Experimentally, the correlation function is defined as $C(k^*) = \xi(k^*) \otimes [N_{\text{same}}(k^*)/N_{\text{mixed}}(k^*)]$, where $\xi(k^*)$ denotes the corrections for experimental effects (see the Appendix for details), $N_{\text{same}}(k^*)$ is the number of detected particle pairs in a given k^* interval obtained by combining particles produced in the same collision (event), which constitute a sample of correlated pairs, and $N_{\text{mixed}}(k^*)$ is the number of uncorrelated pairs in the same k^* interval obtained by combining particles produced in different collisions (mixed events). In this work, the interest resides in studying the final-state interaction for K^+-d and p-d pairs produced in pp collisions at $\sqrt{s} = 13$ TeV. The analyzed dataset is collected using an online trigger to select high-multiplicity pp collisions to enhance the pair sample size. Kaon (K^+), antikaon (K^-), proton (p), antiproton ($\bar{p}$), deuteron (d), and antideuteron ($\bar{d}$) tracks are reconstructed with the ALICE detector, and their momentum in the laboratory frame p is measured in the range $p \in [0.2, 4.1]$ GeV/c. The particle identification is carried out using measurements of the specific energy loss in a time-projection chamber (TPC) and time-of-flight (TOF) detector, resulting in samples of K^+ (K^-), p ($\bar{p}$), d ($\bar{d}$) with a purity of 99.8% (99.8%), 98.2% (97.9%), and 100% (100%), respectively, as estimated via Monte Carlo simulations. Details on the experimental methods and the evaluation of the systematic uncertainties are described in the Appendix. Once the kaons, protons, and deuterons (and charge conjugates) are selected and their three-momenta measured, the correlation functions can be built. Since it is assumed that the same interaction governs hadron-

hadron and antihadron-antihadron pairs [33], in the following, the sum of particles and antiparticles is considered (K^+-$d \equiv K^+$-$d \oplus K^-$-$\bar{d}$ and p-$d \equiv p$-$d \oplus \bar{p} - \bar{d}$).

Figure 1 shows the K^+-d (left panel) and p-d (right panel) correlation functions as a function of k^* measured in pp collisions at $\sqrt{s} = 13$ TeV with ALICE. Both correlation functions are below unity for values of k^* smaller than 200 MeV/c, indicating an overall repulsive interaction. The measured correlation functions are compared to calculations performed using the LL approximation considering either only the Coulomb interaction or, in addition, the strong interaction part determined by the scattering parameters reported in Table I for the K^+-d and p-d systems. In order to compare the experimental data to the LL calculations, the source term included in the formula of the correlation function and the feed-down corrections due to particle decays and residual background contributions are needed to match the experimental measurements.

The source term has been approximated as a Gaussian distribution, whose width defining the source size needs to be evaluated. The values of the p-d and K^+-d source sizes have been obtained from the results of independent analyses of p-p, K^+-p, and π-π correlations, which have demonstrated the existence of a universal source for any hadron-hadron pair in pp collisions at the LHC [40,64] and have indicated that the source size decreases with an increasing value of the pair transverse mass m_{T} (see the Appendix). In addition, further modifications of the source distribution due to strong decays of short-lived resonances decaying into protons and kaons have been taken into account. For p-d pairs, an effective source size of $r_{\text{eff}}^{p\text{-}d} = 1.08 \pm 0.06$ fm has been obtained. For the K^+-d

pairs, the contribution of broad resonances with very different decay times has been taken into account, and the effective source has resulted in $r_{\mathrm{eff}}^{K^+\text{-}d} = 1.35^{+0.04}_{-0.05}$ fm. Note that such small source sizes imply that the most probable distance between particles is around 2 fm [65].

The calculated correlation functions using the LL method shown by the colored bands in Fig. 1 have been corrected for feed-down from weak and strong decays and residual background contributions, using the data-driven methods described in Refs. [33,66], respectively. The relative contributions from primarily produced K^+-d and p-d pairs to the corresponding inclusive sample have been obtained experimentally and are 0.92 and 0.82, respectively. The residual background contribution is shown as the gray-colored band close to unity. The width of the theoretical bands stems from the uncertainty propagation of the experimental determination of the source size, feed-down, and residual background. Additional information on the source size and the different contributions to the correlation function is provided in the Appendix.

The measured K^+-d correlation function is lower than the Coulomb-only prediction showing the presence of a repulsive strong interaction. The calculations with the LL approximation using both sets of scattering parameters (ER and FCA) provide an excellent description of the experimental correlation function within uncertainties. Indeed, since both the Coulomb and the strong K^+-d interactions are repulsive at any distance and there is no feature of the strong interaction that manifests only at very short distances, an asymptotic description is sufficient to reproduce the data. Additionally, kaons are bosons, and the proton and neutron that constitute the deuteron are fermions; hence, the LL approximation of pointlike and distinguishable particles is pertinent, and the properties of the deuteron are mapped in the K^+-d scattering parameters. Hence, given a known interaction and the precise ALICE data, from the expression $C(k^*) = \int d^3 r^* S(r^*) |\psi(\mathbf{k}^*, \mathbf{r}^*)|^2$, one can estimate the source function, even when deuterons are at play. The agreement between the model and the data obtained for the small radius ($r_{\mathrm{eff}}^{K^+\text{-}d} = 1.35^{+0.04}_{-0.05}$ fm) that follows the same m_{T} scaling as all other hadron pairs shows that deuterons are produced at small distances with respect to other hadrons in pp collisions at the LHC, and this result provides an excellent reference for the source term of correlations involving deuterons.

Instead, a huge discrepancy is observed when comparing the p-d data to analogous calculations which consider protons and deuterons as distinguishable pointlike particles and employing the small source size obtained from the m_{T} scaling. This discrepancy can be seen by comparing the measured p-d correlation in the right panel of Fig. 1 to the five different blue shaded curves which are obtained using the five sets of scattering lengths reported in Table I.

The limitations of the LL approximation in describing in detail the p-d interaction are several. The existence of the

^{3}He bound state introduces a particular short-range behavior in the doublet state due to orthogonality requirements. Moreover, the spin structure of the quartet state is completely symmetric, implying as well a specific short-range behavior of the corresponding spatial part to fulfill the requirements of the Pauli principle. In addition, the correct antisymmetrization of the wave function is not considered in the LL approximation, and such short-range features of the interactions are not taken into account. On the other hand, the correlation function obtained with the Coulomb-only assumption (green curve in the right panel of Fig. 1) catches the correct amplitude of the experimental p-d correlation function despite the sizable scattering parameters reported in Table I. This apparent mismatch is due to the fact that in this case, the Coulomb repulsion between the proton and the deuteron reduces the impact of the short-range part of the wave function in the correlation function, and the three-fermion system is not correctly treated within the LL approximation even if only the Coulomb interaction is considered.

III. CORRELATION FUNCTION OF A THREE-BODY SYSTEM

In order to correctly describe the three-body system p-(pn), the microscopic p-d wave function must be employed in the calculation of the p-d correlation function. The latter has been obtained by projecting the p-d wave functions on the initial three-nucleon state created after the pp collisions. The relevant source term in this calculation depends on an effective nucleon-nucleon source radius r_{eff}^{NN} [67,68], since the single nucleons are the relevant degrees of freedom. Details of the calculation are presented in the Appendix and in Ref. [69].

Three different versions of the p-d wave function have been investigated to study the microscopic behavior of the p-d system. First, a Born approximation of the p-d wave function that contains the correct antisymmetrization for the p-(pn) system but where the short-range contribution of the wave function has been omitted. Hence, this calculation accounts only for the asymptotic part of the wave function similar to the LL model but considers the microscopic structure of the p-d system.

The left panel of Fig. 2 shows how the Born approximation compares to the experimental data, including n_σ values that quantify the data-model deviation. It can be seen that this calculation is not sufficiently accurate to reproduce the data, although the antisymmetrization is correctly accounted for. For k^* below 60 MeV/c, this calculation predicts nonphysical values, and therefore they are excluded from the figure. In the same panel, the comparison to the full-fledged Coulomb-only calculation considering the dynamics of three nucleons in the p-d system is shown as well, indicating also a clear disagreement with the data.
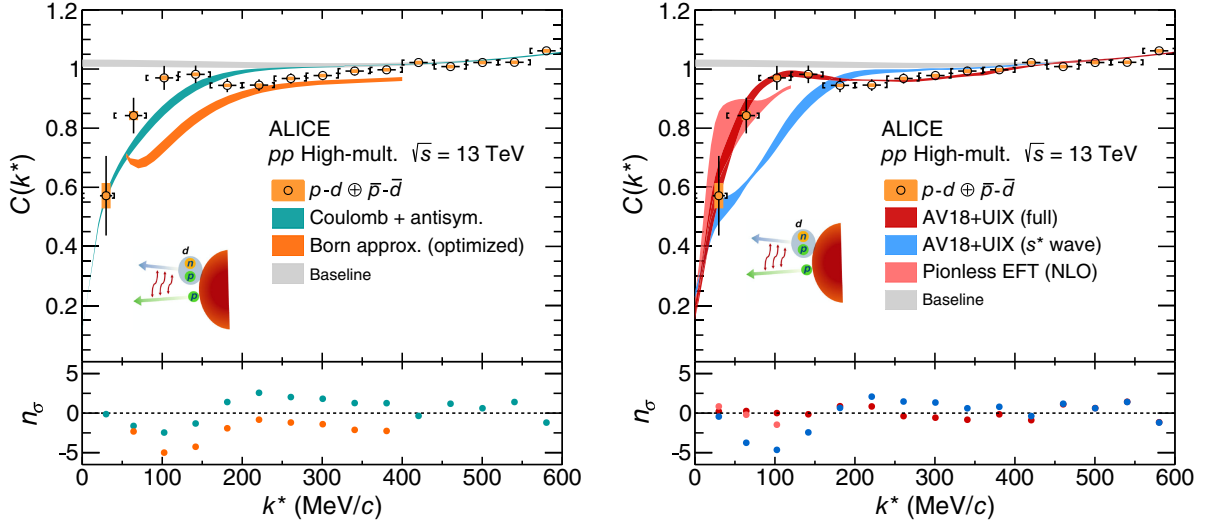
FIG. 2. Measured p-d correlation function plotted as a function of the p-d relative momentum k^* alongside theoretical calculations. The experimental data are represented by circular symbols. The black vertical bars and orange boxes correspond to the statistical and systematic uncertainties, respectively. The square brackets indicate the measurement bin width, and the horizontal black lines represent the statistical uncertainty in the determination of the mean k^* for each bin. The nonfemtoscopic background contributions are represented by the gray band of the cubic baseline. Left panel: the orange and turquoise bands depict calculations obtained using an optimized Born approximation and Coulomb + antisymmetrization of the three-particle wave function, respectively. Right panel: The dark red band represents a fit of the modeled correlation calculated considering p-d as a three-body system with all relevant partial waves (see text). The blue-colored band corresponds to a calculation that includes only $J^\pi = \frac{1}{2}^+, \frac{3}{2}^+$ partial waves relative to the p-d system, which are dominated by the s-wave contributions [69] and thus labeled with s^*. The light red band represents a calculation of the correlation function using pionless EFT at next-to-leading order (see text). All calculations are multiplied by the cubic baseline, and the bandwidths of all calculations account for uncertainties in the determination of the radius and residual contributions. The lower panels present the difference between the measured and calculated correlation function expressed as the number of standard deviations n_σ taking into account the statistical uncertainties of the data and the model uncertainties.

The second wave function that has been tested has been obtained employing the hyperspherical harmonics (HH) method [16]. It accounts for all the relevant two- and three-body interactions at work in the p-(pn) system for the short and the asymptotic range, it accurately describes the three-body dynamics, and it is calculated using p-d scattering observables [16–18]. The nuclear interaction includes the AV18 two-nucleon (NN) [6] plus the Urbana IX (UIX) three-nucleon (NNN) [8] and the Coulomb potentials. The blue curve in the right panel of Fig. 2 has been obtained by including the NN and NNN interactions only in the $J^\pi = \frac{1}{2}^+, \frac{3}{2}^+$ partial waves relative to the p-d system, which are dominated by the s-wave contributions [69]. The n_σ distribution in the lower panel shows that this calculation describes the data moderately well but fails in the small relative momentum part. The agreement improves when more partial waves up to $J^\pi = \frac{7}{2}^-$ are included in the calculation, where the p wave contribute predominantly, as it is shown by the red curve of the right panel of Fig. 2. The correlation function from the full calculation is multiplied by a baseline (gray curve in Fig. 2) that describes the residual background. The parameters of the baseline are obtained by fitting the data and driven by the large-k^* region; see the Appendix for details. The same background is used

for the comparison of the other calculations, and the curves' widths represent the propagated uncertainty of the source parameter and baseline. The full calculation describes the experimental data very accurately, as indicated by the n_σ values for the red band remaining consistently close to or below 1 across the entire range of k^*.

As an additional check, the light red band in the right panel of Fig. 2 shows the p-d correlation function calculated in pionless effective field theory [70] (pionless EFT) calculation at next-to-leading order (NLO). The nuclear interaction within this approach is much simpler than the AV18 + UIX potential [69]; the NN interaction is determined by only the s-wave NN scattering lengths and effective ranges up to NLO, while the NNN interaction is fixed by either the ^{3}H binding energy or the n-d s-wave scattering length. For the pionless EFT calculation, the additional uncertainty from truncating the EFT expansion at NLO can be estimated as 10%. Taking this into account, in the regime where the theory is applicable (k^* below the pion mass of approximately 140 MeV/c), the pionless EFT results are largely compatible with the HH calculation using the AV18 + UIX force.

The fact that the experimental p-d correlation function can be described only by a full-fledged calculation of a

three-body system that considers the single nucleons as active degrees of freedom and that the shape of the correlation function is also sensitive to the inclusion of different partial waves in the interaction demonstrates for the first time that deuteron-proton correlations measured in pp collisions at the LHC access the three-nucleon system at short distances. Indeed, past measurements of correlations involving deuterons [20–23] have been interpreted by means of the LL calculation combined with a value of the source radius larger than the one found for other hadron-hadron pairs in the same colliding system. This misinterpretation of the data was caused by the lack of correct microscopic calculations of the p-d system. It has to be observed that the current formulation of the correlation function does not guarantee invariance under unitarity transformations for distances below 1 fm, and hence, the sensitivity of the observable is limited to the range $r^* > 1$ fm. For the specific dataset analyzed in this work, the distances obtained for the pair of interest are mostly above 1.5 fm.

In order to test the sensitivity of the p-d correlation function to genuine three-baryon interactions, the full-fledged p-d calculation has been carried out excluding such interactions [69]. Figure 3 shows the ratio of the calculated p-d correlation with the AV18 + UIX interactions to the calculation including only the AV18 NN interactions evaluated for different values of the two-nucleon source size r_{eff}^{NN}. The current precision of the data does not allow for testing such effects. However, this will be possible on the larger data samples that will be collected during the LHC Run 3 (2022–2025) with the ALICE upgraded apparatus
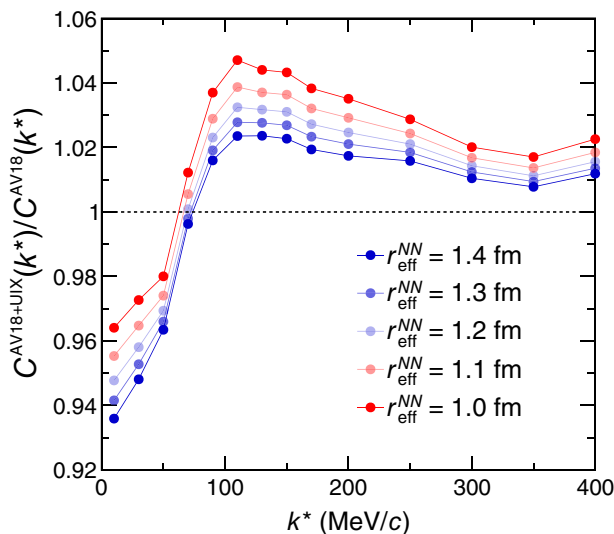
[71]. The integrated luminosity will be increased by 1 order of magnitude with respect to the dataset used in the current work [72]; such an enhancement not only allows us to achieve precision below 1%, similar to the case of the two-body correlation p-Λ [66], but also the differential study of the interaction at small distances by triggering on p-d pairs with large-m_{T} values. Such studies can also be extended to systems such Λ/Σ-d or Λ_c^+-d to investigate three-baryon systems in the strange and charm sectors which are otherwise inaccessible. A combined analysis of p-Λ and Λ-d systems will enable new experimental access to the isospin-dependent hyperon-nucleon interaction.

FIG. 3. Ratio of theoretical p-d correlation functions obtained with full three-body calculations (AV18 for NN + UIX for NNN interaction) to those obtained using an AV18 for NN interaction only for different values of the two-nucleon effective source size r_{eff}^{NN}.

APPENDIX: METHODS

1. Event selection

A data sample of inelastic pp collisions at $\sqrt{s} = 13$ TeV was recorded with ALICE [73,74] at the LHC. General details on the event selection, pile-up rejection, and the primary vertex reconstruction can be found in Ref. [75]. A trigger that requires the total signal amplitude measured in the V0 detector [76] to exceed a certain threshold was employed to select high-multiplicity (HM) events. The V0 detector comprises two plastic scintillator arrays placed on both sides of the interaction point at pseudorapidities $2.8 < \eta < 5.1$ and $-3.7 < \eta < -1.7$. The pseudorapidity is defined as $\eta = -\ln[\tan(\theta/2)]$, where θ is the polar angle of the particle with respect to the proton beam axis.

At $\sqrt{s} = 13$ TeV, the average number of charged particles produced in HM events in the range $|\eta| < 0.5$ is 30. This η range corresponds to the region within (26°) of the transverse plane perpendicular to the beam axis. The HM events constitute only 0.17% of the pp collisions that produce at least one charged particle in the pseudorapidity range $|\eta| < 1.0$. A total of 1×10^9 HM events were analyzed. Additional details on the HM event selection can be found in Ref. [75].

2. Particle tracking and identification

For the identification and momentum measurement of charged particles, the Inner Tracking System (ITS) [77], TPC [78], and TOF [79] detectors of ALICE are employed. All three detectors are located inside a uniform magnetic field generated by the L3 solenoid (0.5 T), leading to a bending of the trajectories of charged particles. The measurement of the curvature is used to reconstruct the particle momenta. Typical transverse-momentum (p_T) resolutions for kaons, protons, and deuterons vary from about 2% for tracks with $p_T = 10$ GeV/c to below 1% for $p_T < 1$ GeV/c. The particle identity is determined by the energy lost per unit of track length inside the TPC detector and by the particle velocity measured in the TOF detector. For additional experimental details, see Ref. [74]. Basic details on the selection criteria of the proton, kaon, and deuteron tracks used in this work can be found in Ref. [80].

Kaons are identified via the measurement of the specific energy loss in TPC within a momentum range $p \in [0.2, 2.0]$ GeV/c. This information is combined with the time-of-flight measurement for momentum $p > 0.4$ GeV/c. In the kaon sample, the contamination from electrons produced via photon conversion in the detector material is removed by excluding kaon candidates in the momentum range $0.5 < p < 0.65$ GeV/c. The selected candidates that simultaneously fulfill the selection criteria of the pion (using TPC and TOF information) or proton (using TPC information) are also excluded from the sample.

Protons are selected within a transverse-momentum range of $0.5 < p_T < 4.05$ GeV/c. They are identified by requiring TPC information for candidate tracks with momentum $p < 0.75$ GeV/c, while TPC and TOF information are both required for candidates with $p > 0.75$ GeV/c. The identification of deuterons is performed with the TPC in the momentum range $0.4 < p < 1.4$ GeV/c. For the analysis of K^+-d pairs, the deuteron acceptance is extended by using TOF identification in the region $1.4 < p < 2.3$ GeV/c.

The selection of kaons, protons, and deuterons constitute the main source of systematic uncertainties associated with the measured correlation function. All particle selection criteria are varied with respect to their default values. In order to account for the effect of possible correlations, the analysis of K^+-d (p-d) pairs is repeated 40 (44) times using random combinations of such selection criteria. The associated systematic uncertainty of the measured correlation function for each k^* point is given by the root-mean-square of all 40 (44) resulting correlation functions. The total systematic uncertainties are maximal at low k^*, reaching a value of 3% and 7% for K^+-d and p-d, correspondingly.

3. Characterization of the source of particles

The distribution $S(r^*)$ of the distance r^* at which particles are emitted is described by a Gaussian function whose width characterizes the source size. In Ref. [40], the baryon-baryon source sizes are determined as a function of the transverse mass of the baryon-baryon pair $m_T = (k_T{}^2 + m^2)^{1/2}$, where m is the average mass, and $k_T = |\mathbf{p}_{T,1} + \mathbf{p}_{T,2}|/2$ is the transverse momentum of the pair. For p-d and K^+-d pairs, it is assumed that the common source for all baryons still holds for any hadron-hadron pair [40]. The measured $\langle m_T \rangle$ for p-d and K^+-d pairs are 1.64 and 1.50 GeV/c, respectively, implying source sizes of $r_{\mathrm{core}}^{K^+\text{-}d} = 1.04 \pm 0.04$ fm and $r_{\mathrm{core}}^{p\text{-}d} = 0.99 \pm 0.05$ fm, where r_{core} denotes the width of the Gaussian distribution defining

the source before taking into account the effect produced by short-lived resonances.

In pp collisions at $\sqrt{s} = 13$ TeV, about 2/3 of the protons and 1/3 of the kaons originate from the decay of short-lived resonances with a lifetime ($c\tau$) of a few fm. Table II shows the major relative contributions to the proton and kaon samples by several resonances, according to statistical hadronization [81]. The effect of such resonances on the source size is evaluated by folding the Gaussian source with an exponential distribution containing the resonance decay constant, following Ref. [40]. The resulting source distribution for p-d can be parametrized with an effective Gaussian source radius equal to $r_{\mathrm{eff}}^{p\text{-}d} = 1.08 \pm 0.06$ fm. For K^+-d pairs, the resulting source distribution is described using a sum of two Gaussian functions with radii 1.10 ± 0.04 and $2.14_{-0.07}^{+0.03}$ fm with weights of 0.76 and 0.24, respectively. The effective source size quoted in the text $r_{\mathrm{eff}}^{K^+\text{-}d} = 1.35_{-0.05}^{+0.04}$ fm results from the weighted sum of the two Gaussians. Note that a description with a single Gaussian (1G) for the K^+-d source distribution, including the effects of resonances is not satisfactory, but it is nevertheless illustrative to compare the resulting radius of $r_{\mathrm{eff1G}}^{K^+\text{-}d} = 1.22 \pm 0.04$ fm with the p-d radius $r_{\mathrm{eff}}^{p\text{-}d} = 1.08 \pm 0.06$ fm.

In the case of the three-body calculation for the p-d system, the formalism requires as input the two-particle source size for each pairwise source of the p-(pn) system. For nucleon pairs, an average core source size of $r_{\mathrm{core}}^{NN} = 1.35 \pm 0.14$ fm is estimated using the measured $\langle m_T \rangle$ for p-d and the measured $\langle p_T \rangle$ of deuteron and protons below $k^* < 400$ MeV/c. The source size r_{core}^{NN} is enhanced by the strongly decaying resonances that feed to protons and neutrons. Similar to the case of p-d and K^+-d pairs, this effect in the source size is taken into account by folding the Gaussian source with an exponential distribution. The resulting source distribution for NN pairs can be characterized by an effective Gaussian source radius equal to

TABLE II. Fractions of protons and kaons feeding from the strongly decaying short-lived decays of resonances. The contribution of kaons from the $\phi(1020)$ decays are considered as feed-down to the correlation functions.

	Protons			Kaons	
Resonances	$c\tau$ (fm)	Fractions (%)	Resonances	$c\tau$ (fm)	Fractions (%)
Δ^{++}	1.64	21.87	$K^*(892)^0$	3.89	21
Δ^+	1.64	14.60	$K^*(892)^+$	3.88	11
Δ^0	1.64	7.20	$a_0(980)^+$	2.63	1
$N(1440)^0$	0.56	0.91	$K_2^*(1430)^0$	1.81	1
$N(1520)^0$	1.64	1.75	$K_1^*(1270)^0$	2.19	1
$N(1680)^0$	1.52	1.15	$\phi(1020)$	46.32	(6)
$N(1535)^+$	1.31	1.02	$\cdots$	$\cdots$	$\cdots$
$N(1440)^+$	0.56	0.91	$\cdots$	$\cdots$	$\cdots$

$r_{\text{eff}}^{NN} = 1.43_{-0.16}^{+0.16}$ fm. This source size is an average of distances between the p-p and p-n pairs that form the p-d system.

4. Corrections of the correlation function

The experimental correlation function defined as $C(k^*) = \xi(k^*) \otimes [N_{\text{same}}(k^*)/N_{\text{mixed}}(k^*)]$ is corrected via $\xi(k^*)$ for normalization and the unfolding of momentum resolution effects. A normalization factor $\mathcal{N}$ is used to correct for the different yields in same- and mixed-event distributions. The value of the normalization factor is chosen such that the mean value of the correlation function is equal to unity. It is obtained by dividing the integral of the $N_{\text{same}}(k^*)$ and $N_{\text{mixed}}(k^*)$ in a region where the effect of final-state interactions is negligible (for p-d, $200 < k^* < 500$ MeV/c and in the case of K^+-d, $300 < k^* < 600$ MeV/c).

The shape of the measured correlation function is affected by the finite resolution in the determination of the momentum of particles. The measured same- and mixed-event distributions are unfolded for the momentum smearing using Monte Carlo (MC) simulations. The correction for the measured correlation function due to the momentum resolution effect with the MC event generator is found to be at most 3% for p-d and 9% for K^+-d at low k^*. Moreover, the resolution effects due to the merging of trajectories, which cross the detector at a distance comparable with the spatial resolution of the detector (ITS or TPC), are evaluated and found to be negligible.

While the measured p-d and K^+-d correlation functions are dominated by the interaction between p-d and K^+-d pairs consisting of primary particles produced in the collision, they are also influenced by the effects caused by the misidentification of particles and by the contribution of secondary particles produced in weak decays. Because of the large decay times of weakly decaying particles, the final-state interaction between their decay products and the primary particle of interest is absent, thus leading to either a flat contribution or a residual signature of the interaction with the parent hadron. The contributions to $C(k^*)$ from the genuine correlation of primary particles, the misidentified hadrons, and the secondary particles are quantified by the so-called λ parameters, which are computed from the purity and the primary fraction of each particle species as described in Ref. [33]. The λ parameters for the genuine correlation function of p-d and K^+-d are listed in Table III. All residual correlations not stemming from genuine primary pairs in the p-d and K^+-d correlation functions are assumed to be equal to unity regardless of the values of k^*, and the theoretical correlation functions shown in Figs. 1 and 2 are corrected using the corresponding λ parameters.

In addition to the residual correlation, the theoretical correlation function is also corrected for the rising tail effect of the experimental correlation in the region where the final-

TABLE III. λ parameters of the genuine particle pairs for p-d and K^+-d.

λ parameter	Value
λ_{pd}	79.7%
$\lambda_{\bar{p}\bar{d}}$	84.1%
$\lambda_{K^+ d}$	90.1%
$\lambda_{K^- \bar{d}}$	94.1%

state interaction is negligible and that can be originated from effects such as energy conservation. A multiplicative cubic baseline $\text{BL}(k^*) = a + bk^{*2} + ck^{*3}$ is used to describe the data at large k^*. For K^+-d correlations, the baseline is prefitted in the region of $300 < k^* < 1800$ MeV/c. In the case of the p-d correlation function, the parameters a, b, and c are obtained from a fit to the data in the region $0 < k^* < 700$ MeV/c including the theoretical correlation function and the multiplicative baseline. The baseline is represented by the gray bands in Figs. 1 and 2.

The uncertainties on the determination of the residual contributions, the baseline, and the source size are propagated to the theoretical correlation functions and contribute, together with the intrinsic theoretical uncertainties of each model, to the width of the bands shown in Figs. 1 and 2. The main contributions to the total uncertainty are those derived from the baseline fit and the radius determination. The former are evaluated by variations in the limits of the fit range of ± 50 MeV/c for the upper and lower limits in the case of K^+-d, and ± 40 MeV/c in the upper limit for p-d. The uncertainty of the radius is propagated from the uncertainties in the parametrization of the m_{T} scaling according to Ref. [40], and it is of 6.2% (0.1%) and 2% (2%) at $k^* = 50$ (100) MeV/c for the p-d and K^+-d pairs, respectively.

5. The Lednický-Lyuboshitz model

The final-state interaction for two charged pointlike particles has been modeled in Ref. [63]. The definition of the relative s-wave function for a system of two charged pointlike distinguishable particles is given as

$$\psi(\mathbf{k}^*, \mathbf{r}^*) = e^{i\delta_c} \sqrt{A_c(\eta)} \left[e^{-i\mathbf{k}^* \cdot \mathbf{r}^*} F(-i\eta, 1, i\xi) \right.$$
$$\left. + f_C(k^*) \frac{\tilde{G}(\rho, \eta)}{r*} \right], \tag{A1}$$

where $\eta = (k^* a_C)^{-1}$, a_C is the Bohr radius including the sign of the interaction between the pair of particles, $\xi = \rho(1 + \cos(\theta^*))$, and $\rho = k^* r^*$, where θ^* is the angle between $\mathbf{k}^*$ and $\mathbf{r}^*$. The term $A_C(\eta) = 2\pi\eta[\exp(2\pi\eta) - 1]^{-1}$ is a Coulomb-barrier penetration factor, also known as the Gamow factor. The Coulomb interaction (asymptotic form) in the wave function is described by the term

$e^{-i\mathbf{k}^*\cdot\mathbf{r}^*}F(\alpha,1,z)$ together with $\tilde{G}(\rho,\eta)$, where $F(\alpha,1,z) = 1 + (\alpha z/!2) + +[\alpha(\alpha+1)z^2/!2^2] + \cdots$ is a confluent hypergeometric function and $\tilde{G}(\rho,\eta) = \sqrt{Ac}(G_0 + iF_0)$ is a combination of the regular (F_0) and singular (G_0) s-wave Coulomb functions. The strong nuclear interaction is computed using the Coulomb-corrected scattering amplitude f_C defined as

$$f_C(k^*) = \left[\frac{1}{-a_0} + \frac{d_0 k^{*2}}{2} - ik^* A_C(k^*) - \frac{2}{a_C}h(k^*)\right]^{-1}. \tag{A2}$$

The function $h(k^*)$ is written as $h(k^*) = [1/(k^* a_C)^2]\sum_{n=1}^{\infty}[n(n^2 + (k^* a_C)^{-2})]^{-1} - \gamma + \ln|k^* a_C|$, where the constant $\gamma = 0.5772$ is the Euler constant.

6. Three-body formalism for the *p-d* correlation function

In order to account for the internal structure of the deuteron, a calculation of the proton-deuteron correlation function that includes a microscopic *p-d* wave function $\Psi_{m_2,m_1}(\boldsymbol{x},\boldsymbol{y})$ is carried out. This wave function accounts for all the relevant two- and three-body interactions at work in the *p*-(*pn*) system for the short and asymptotic ranges. It accurately describes the three-body dynamics [16–18] since it is tuned on *p-d* scattering observables. The variables $\boldsymbol{x}$ and $\boldsymbol{y}$ are the Jacobi vectors of the system, and they asymptotically denote the distance of the *p-n* system within the deuteron and the *p-d* distance, respectively. The indices m_2 and m_1 are quantum numbers of the spin operators for the deuteron and the proton when they are very well apart. The three-body correlation is calculated using the formalism discussed in Refs. [67,68]. More details about the employed wave functions and the computation of the *p-d* correlation function can be found in Ref. [69]. In general, the formalism is based on the following expressions:

$$C_{pd}(k) = \frac{1}{A_d}\frac{1}{6}\sum_{m_2,m_1}\int d^3r_1 d^3r_2 d^3r_3 S_1(r_1)S_1(r_2)$$
$$\times S_1(r_3)|\Psi_{m_2,m_1}|^2, \tag{A3}$$

$$A_d = \frac{1}{3}\sum_{m_2}\int d^3r_1 d^3r_2 S_1(r_1)S_1(r_2)|\phi_{m_2}|^2, \tag{A4}$$

$$S_1(r) = \frac{1}{(2\pi R_M^2)^{\frac{3}{2}}}e^{-r^2/2R_M^2}, \tag{A5}$$

where ϕ_{m_2} is the deuteron wave function, and $S_1(r)$ represents the single particle source term of radius R_M, while the factor 6 in the denominator of Eq. (A3) takes into account the possible spin configurations. The quantity A_d can be related to the probability of deuteron formation in

the reaction. Note that in this calculation, the accurate *p-d* wave function is different from the approximated form employed in Refs. [67,68]. By considering a suitable choice of coordinates, one can demonstrate [19] that the parameter R_M corresponds to the effective radius for the two-nucleon system. For the *p-d* system, R_M is estimated considering the measured $\langle m_T\rangle$ of the *p-d* pairs and the average transverse momentum $\langle p_T\rangle$ of the deuterons and protons used for the correlation. The value $R_M = r_{\text{eff}}^{NN} = 1.43^{+0.16}_{-0.16}$ fm is obtained and used in the calculation.

[1] H.-W. Hammer, A. Nogga, and A. Schwenk, *Three-body forces: From cold atoms to nuclei*, Rev. Mod. Phys. **85**, 197 (2013).

[2] H. Hergert, *A guided tour of ab initio nuclear many-body theory*, Front. Phys. **8**, 379 (2020).

[3] J. Lynn, I. Tews, S. Gandolfi, and A. Lovato, *Quantum Monte Carlo methods in nuclear physics: Recent advances*, Annu. Rev. Nucl. Part. Sci. **69**, 279 (2019).

[4] M. Baldo, G. F. Burgio, and I. Bombaci, *Microscopic nuclear equation of state with three-body forces and neutron star structure*, Astron. Astrophys. **328**, 274 (1997), https://ui.adsabs.harvard.edu/abs/1997A%26A.. .328..274B/abstract.

[5] I. Bombaci and D. Logoteta, *Equation of state of dense nuclear matter and neutron star structure from nuclear chiral interactions*, Astron. Astrophys. **609**, A128 (2018).

[6] R. B. Wiringa, V. G. J. Stoks, and R. Schiavilla, *Accurate nucleon-nucleon potential with charge-independence breaking*, Phys. Rev. C **51**, 38 (1995).

[7] V. G. J. Stoks, R. A. M. Klomp, C. P. F. Terheggen, and J. J. de Swart, *Construction of high quality NN potential models*, Phys. Rev. C **49**, 2950 (1994).

[8] B. S. Pudliner, V. R. Pandharipande, J. Carlson, S. C. Pieper, and R. B. Wiringa, *Quantum Monte Carlo calculations of nuclei with A ≤ 7*, Phys. Rev. C **56**, 1720 (1997).

[9] S. A. Coon and H. K. Han, *Reworking the Tucson-Melbourne three nucleon potential*, Few Body Syst. **30**, 131 (2001).

[10] E. Epelbaum, H. Krebs, and P. Reinert, *High-precision nuclear forces from chiral EFT: State-of-the-art, challenges and outlook*, Front. Phys. **8**, 98 (2020).

[11] E. Epelbaum *et al.* (LENPIC Collaboration), *Few- and many-nucleon systems with semilocal coordinate-space regularized chiral two- and three-body forces*, Phys. Rev. C **99**, 024313 (2019).

[12] M. Piarulli *et al.*, *Light-nuclei spectra from chiral dynamics*, Phys. Rev. Lett. **120**, 052503 (2018).

[13] M. Piarulli, L. Girlanda, R. Schiavilla, A. Kievsky, A. Lovato, L. E. Marcucci, S. C. Pieper, M. Viviani, and R. B. Wiringa, *Local chiral potentials with Δ-intermediate states and the structure of light nuclei*, Phys. Rev. C **94**, 054007 (2016).

[14] P. Reinert, H. Krebs, and E. Epelbaum, *Semilocal momentum-space regularized chiral two-nucleon potentials up to fifth order*, Eur. Phys. J. A **54**, 86 (2018).

[15] S. K. Saha, D. R. Entem, R. Machleidt, and Y. Nosyk, *Local position-space two-nucleon potentials from leading to fourth order of chiral effective field theory*, Phys. Rev. C **107**, 034002 (2023).

[16] A. Kievsky, M. Viviani, and S. Rosati, *Polarization observables in p-d scattering below 30 MeV*, Phys. Rev. C **64**, 024002 (2001).

[17] A. Kievsky, M. Viviani, and L. E. Marcucci, *N-d scattering including electromagnetic forces*, Phys. Rev. C **69**, 014002 (2004).

[18] A. Deltuva, A. C. Fonseca, A. Kievsky, S. Rosati, P. U. Sauer, and M. Viviani, *Benchmark calculation for proton-deuteron elastic scattering observables including Coulomb*, Phys. Rev. C **71**, 064003 (2005).

[19] S. Mrówczyński and P. Słoń, *Hadron-deuteron correlations and production of light nuclei in relativistic heavy-ion collisions*, Acta Phys. Pol. B **51**, 1739 (2020).

[20] C. B. Chitwood *et al.*, *Final-state interactions between noncompound light particles for ^{16}O-induced reactions on ^{197}Au at $E/A = 25$ MeV*, Phys. Rev. Lett. **54**, 302 (1985).

[21] J. Pochodzalla *et al.*, *External Coulomb distortion of proton-deuteron final-state interactions for induced reactions on Au at $E/A = 35$ MeV*, Phys. Lett. B **175**, 275 (1986).

[22] J. Pochodzalla *et al.*, *Two-particle correlations at small relative momenta for ^{40}induced reactions on ^{197}Au at $E/A = 60$ MeV*, Phys. Rev. C **35**, 1695 (1987).

[23] K. Wosińska *et al.*, *Correlations of neutral and charged particles in ^{40}Ar-^{58}Ni reaction at 77 MeV/u*, Eur. Phys. J. A **32**, 55 (2007).

[24] V. T. Cocconi, T. Fazzini, G. Fidecaro, M. Legros, N. H. Lipman, and A. W. Merrison, *Mass analysis of the secondary particles produced by the 25-GeV proton beam of the Cern Proton Synchrotron*, Phys. Rev. Lett. **5**, 19 (1960).

[25] S. Nagamiya, *Experimental overview*, Nucl. Phys. **A544**, 5 (1992).

[26] C. Adler *et al.* (STAR Collaboration), *Anti-deuteron and anti-He-3 production in $\sqrt{s_{NN}} = 130$ GeV Au + Au collisions*, Phys. Rev. Lett. **87**, 262301 (2001); **87**, 279902(E) (2001).

[27] S. S. Adler *et al.* (PHENIX Collaboration), *Deuteron and antideuteron production in Au + Au collisions at $\sqrt{s_{NN}} = 200$ GeV*, Phys. Rev. Lett. **94**, 122302 (2005).

[28] H. Agakishiev *et al.* (STAR Collaboration), *Observation of the antimatter helium-4 nucleus*, Nature (London) **473**, 353 (2011); **475**, 412(E) (2011).

[29] S. Acharya *et al.* (ALICE Collaboration), *Production of deuterons, tritons, ^{3}He nuclei and their antinuclei in pp collisions at $\sqrt{s} = 0.9$, 2.76 and 7 TeV*, Phys. Rev. C **97**, 024615 (2018).

[30] J. Adam *et al.* (ALICE Collaboration), *Production of light nuclei and anti-nuclei in pp and Pb − Pb collisions at energies available at the CERN Large Hadron Collider*, Phys. Rev. C **93**, 024917 (2016).

[31] S. Acharya *et al.* (ALICE Collaboration), *(Anti-)deuteron production in pp collisions at $\sqrt{s} = 13$ TeV*, Eur. Phys. J. C **80**, 889 (2020).

[32] S. Acharya *et al.* (ALICE Collaboration), *Measurement of deuteron spectra and elliptic flow in Pb-Pb collisions at $\sqrt{s_{NN}} = 2.76$ TeV at the LHC*, Eur. Phys. J. C **77**, 658 (2017).

[33] S. Acharya *et al.* (ALICE Collaboration), *$p − p$, $p − \Lambda$ and $\Lambda − \Lambda$ correlations studied via femtoscopy in pp reactions at $\sqrt{s} = 7$ TeV*, Phys. Rev. C **99**, 024001 (2019).

[34] S. Acharya *et al.* (ALICE Collaboration), *First observation of an attractive interaction between a proton and a cascade baryon*, Phys. Rev. Lett. **123**, 112002 (2019).

[35] S. Acharya *et al.* (ALICE Collaboration), *Scattering studies with low-energy kaon-proton femtoscopy in proton-proton collisions at the LHC*, Phys. Rev. Lett. **124**, 092301 (2020).

[36] S. Acharya *et al.* (ALICE Collaboration), *Unveiling the strong interaction among hadrons at the LHC*, Nature (London) **588**, 232 (2020).

[37] S. Acharya *et al.* (ALICE Collaboration), *Experimental evidence for an attractive p-ϕ interaction*, Phys. Rev. Lett. **127**, 172301 (2021).

[38] S. Acharya *et al.* (ALICE Collaboration), *First study of the two-body scattering involving charm hadrons*, Phys. Rev. D **106**, 052010 (2022).

[39] S. Acharya *et al.* (ALICE Collaboration), *Kaon-proton strong interaction at low relative momentum via femtoscopy in Pb − Pb collisions at the LHC*, Phys. Lett. B **822**, 136708 (2021).

[40] S. Acharya *et al.* (ALICE Collaboration), *Search for a common baryon source in high-multiplicity pp collisions at the LHC*, Phys. Lett. B **811**, 135849 (2020).

[41] A. Feliciello and T. Nagae, *Experimental review of hypernuclear physics: recent achievements and future perspectives*, Rep. Prog. Phys. **78**, 096301 (2015).

[42] L. Tolos and L. Fabbietti, *Strangeness in nuclei and neutron stars*, Prog. Part. Nucl. Phys. **112**, 103770 (2020).

[43] T. R. Saito *et al.*, *New directions in hypernuclear physics*, Nat. Rev. Phys. **3**, 803 (2021).

[44] J. Rowley *et al.* (CLAS Collaboration), *Improved Λp elastic scattering cross sections between 0.9 and 2.0 GeV/c as a main ingredient of the neutron star equation of state*, Phys. Rev. Lett. **127**, 272303 (2021).

[45] L. Fabbietti, V. Mantovani Sarti, and O. Vazquez Doce, *Study of the strong interaction among hadrons with correlations at the LHC*, Annu. Rev. Nucl. Part. Sci. **71**, 377 (2021).

[46] S. Acharya *et al.* (ALICE Collaboration), *The ALICE experiment—A journey through QCD*, Eur. Phys. J. C **84**, 813 (2024).

[47] L. D. Knutson, L. O. Lamm, and J. E. McAninch, *Determination of the phase shifts for p-d elastic scattering at $E_p = 3$ MeV*, Phys. Rev. Lett. **71**, 3762 (1993).

[48] R. Sherr *et al.*, *Scattering of protons by deuterons*, Phys. Rev. **72**, 662 (1947).

[49] C. Brune *et al.*, *Possible three-nucleon force effects in d-p scattering at low energies*, Phys. Lett. B **428**, 13 (1998).

[50] E. Huttel, W. Arnold, H. Berg, H. Krause, J. Ulbricht, and G. Clausnitzer, *Differential cross sections and analyzing powers for pd elastic scattering below 1.0 MeV*, Nucl. Phys. **A406**, 435 (1983).

[51] T. Clegg *et al.*, *A new atomic beam polarized ion source for the triangle universities nuclear laboratory: Overview, operating experience, and performance*, Nucl. Instrum. Methods Phys. Res., Sect. A **357**, 200 (1995).

[52] T. Takaki, *Optical potential approach to K + d scattering at low energies*, Phys. Rev. C **81**, 055204 (2010).

[53] K. Aoki and D. Jido, *KN scattering amplitude revisited in a chiral unitary approach and a possible broad resonance in S = +1 channel*, Prog. Theor. Exp. Phys. **2019**, 013D01 (2019).

[54] S. S. Kamalov, E. Oset, and A. Ramos, *Chiral unitary approach to the K-deuteron scattering length*, Nucl. Phys. **A690**, 494 (2001).

[55] J. Arvieux, *Phase-shift analysis of elastic proton-deuteron scattering cross sections and ^{3}He excited states*, Nucl. Phys. **A221**, 253 (1974).

[56] W. T. H. Van Oers *et al.*, *Phase-shift analysis of elastic nucleon-deuteron scattering*, Nucl. Phys. **A92**, 561 (1967).

[57] E. Huttel *et al.*, *Phase-shift analysis of p-d elastic scattering below break-up threshold*, Nucl. Phys. **A406**, 443 (1983).

[58] A. Kievsky *et al.*, *The three nucleon system near the N-d threshold*, Phys. Lett. B **406**, 292 (1997).

[59] T. C. Black *et al.*, *Determination of proton-deuteron scattering lengths*, Phys. Lett. B **471**, 103 (1999).

[60] S. Pratt, *Pion interferometry of quark-gluon plasma*, Phys. Rev. D **33**, 1314 (1986).

[61] M. Lisa *et al.*, *Femtoscopy in relativistic heavy-ion collisions*, Annu. Rev. Nucl. Part. Sci. **55**, 357 (2005).

[62] R. Lednicky and V. L. Lyuboshits, *Final state interaction effect on pairing correlations between particles with small relative momenta*, Yad. Fiz. **35**, 1316 (1981) [R. Lednicky and V. L. LyuboshitsSov. J. Nucl. Phys. **35**, 770 (1982)], https://inspirehep.net/literature/167537.

[63] R. Lednicky, *Finite-size effects on two-particle production in continuous and discrete spectrum*, Phys. Part. Nucl. **40**, 307 (2009).

[64] S. Acharya *et al.* (ALICE Collaboration), *Common femtoscopic hadron-emission source in pp collisions at the LHC*, arXiv:2311.14527.

[65] D. Mihaylov, V. Mantovani Sarti, O. Arnold, L. Fabbietti, B. Hohlweger, and A. Mathis, *A femtoscopic correlation analysis tool using the Schrödinger equation (CATS)*, Eur. Phys. J. C **78**, 394 (2018).

[66] S. Acharya *et al.* (ALICE Collaboration), *Exploring the $N\Lambda - N\Sigma$ coupled system with high precision correlation techniques at the LHC*, Phys. Lett. B **833**, 137272 (2022).

[67] S. Mrówczyński, *Production of light nuclei at colliders—coalescence vs. thermal model*, Eur. Phys. J. Special Topics **229**, 3559 (2020).

[68] S. Mrówczyński and P. Słoń, *Deuteron-deuteron correlation function in nucleus-nucleus collisions*, Phys. Rev. C **104**, 024909 (2021).

[69] M. Viviani, S. König, A. Kievsky, L. E. Marcucci, B. Singh, and O. Vázquez Doce, *Role of three-body dynamics in nucleon-deuteron correlation functions*, Phys. Rev. C **108**, 064002 (2023).

[70] H.-W. Hammer, S. König, and U. van Kolck, *Nuclear effective field theory: Status and perspectives*, Rev. Mod. Phys. **92**, 025004 (2020).

[71] S. Acharya *et al.* (ALICE Collaboration), *ALICE upgrades during the LHC Long Shutdown 2*, J. Instrum. **19**, P05062 (2024).

[72] Z. Citron *et al.*, *Report from Working Group 5: Future physics opportunities for high-density QCD at the LHC with heavy-ion and proton beams*, CERN Yellow Rep. Monogr. **7**, 1159 (2019).

[73] K. Aamodt *et al.* (ALICE Collaboration), *The ALICE experiment at the CERN LHC*, J. Instrum. **3**, S08002 (2008).

[74] B. Abelev *et al.* (ALICE Collaboration), *Performance of the ALICE Experiment at the CERN LHC*, Int. J. Mod. Phys. A **29**, 1430044 (2014).

[75] S. Acharya *et al.* (ALICE Collaboration), *Investigation of the p-Σ^0 interaction via femtoscopy in pp collisions*, Phys. Lett. B **805**, 135419 (2020).

[76] E. Abbas *et al.* (ALICE Collaboration), *Performance of the ALICE VZERO system*, J. Instrum. **8**, P10016 (2013).

[77] K. Aamodt *et al.* (ALICE Collaboration), *Alignment of the ALICE Inner Tracking System with cosmic-ray tracks*, J. Instrum. **5**, P03003 (2010).

[78] J. Alme *et al.*, *The ALICE TPC, a large 3-dimensional tracking device with fast readout for ultra-high multiplicity events*, Nucl. Instrum. Methods Phys. Res., Sect. A **622**, 316 (2010).

[79] A. Akindinov *et al.*, *Performance of the ALICE Time-of-Flight detector at the LHC*, Eur. Phys. J. Plus **128**, 44 (2013).

[80] S. Acharya *et al.* (ALICE Collaboration), *Study of the p-p-K^+ and p-p-K^- dynamics using the femtoscopy technique*, Eur. Phys. J. A **59**, 298 (2023).

[81] V. Vovchenko and H. Stoecker, *Thermal-fist: A package for heavy-ion collisions and hadronic equation of state*, Comput. Phys. Commun. **244**, 295 (2019).

S. Acharya,[131] D. Adamová,[90] G. Aglieri Rinella,[35] M. Agnello,[32] N. Agrawal,[54] Z. Ahammed,[139] S. Ahmad,[16] S. U. Ahn,[75] I. Ahuja,[40] A. Akindinov,[146] M. Al-Turany,[101] D. Aleksandrov,[146] B. Alessandro,[60] H. M. Alfanda,[6] R. Alfaro Molina,[71] B. Ali,[16] A. Alici,[28] N. Alizadehvandchali,[120] A. Alkin,[35] J. Alme,[21] G. Alocco,[55] T. Alt,[68] A. R. Altamura,[53] I. Altsybeev,[99] J. R. Alvarado,[47] M. N. Anaam,[6] C. Andrei,[48] N. Andreou,[119] A. Andronic,[130] V. Anguelov,[98] F. Antinori,[57] P. Antonioli,[54] N. Apadula,[78] L. Aphecetche,[107] H. Appelshäuser,[68] C. Arata,[77] S. Arcelli,[28] M. Aresti,[24] R. Arnaldi,[60] J. G. M. C. A. Arneiro,[114] I. C. Arsene,[20] M. Arslandok,[142] A. Augustinus,[35] R. Averbeck,[101] M. D. Azmi,[16] H. Baba,[128] A. Badalà,[56] J. Bae,[108] Y. W. Baek,[43] X. Bai,[124] R. Bailhache,[68] Y. Bailung,[51] A. Balbino,[32] A. Baldisseri,[134] B. Balis,[2] D. Banerjee,[4a,4b] Z. Banoo,[95] R. Barbera,[29] F. Barile,[34a,34b] L. Barioglio,[99] M. Barlou,[82] B. Barman,[44]

G. G. Barnaföldi[49] L. S. Barnby[89] V. Barret[131] L. Barreto[114] C. Bartels[123] K. Barth[35] E. Bartsch[68] N. Bastid[131] S. Basu[79] G. Batigne[107] D. Battistini[99] B. Batyunya[147] D. Bauri,[50] J. L. Bazo Alba[105] I. G. Bearden[87] C. Beattie[142] P. Becht[101] D. Behera[51] I. Belikov[133] A. D. C. Bell Hechavarria[130] F. Bellini[28] R. Bellwied[120] S. Belokurova[146] Y. A. V. Beltran[47] G. Bencedi[49] S. Beole[27] Y. Berdnikov[146] A. Berdnikova[98] L. Bergmann[98] M. G. Besoiu[67] L. Betev[35] P. P. Bhaduri[139] A. Bhasin[95] M. A. Bhat,[4a,4b] B. Bhattacharjee[44] L. Bianchi[27] N. Bianchi[52] J. Bielčík[38] J. Bielčíková[90] J. Biernat[111] A. P. Bigot[133] A. Bilandzic[99] G. Biro[49] S. Biswas,[4a,4b] N. Bize[107] J. T. Blair[112] D. Blau[146] M. B. Blidaru[101] N. Bluhme,[41] C. Blume[68] G. Boca[23,58] F. Bock[91] T. Bodova[21] A. Bogdanov,[146] S. Boi[24] J. Bok[62] L. Boldizsár[49] M. Bombara[40] P. M. Bond[35] G. Bonomi[58,138] H. Borel[134] A. Borissov[146] A. G. Borquez Carcamo[98] H. Bossi[142] E. Botta[27] Y. E. M. Bouziani[68] L. Bratrud[68] P. Braun-Munzinger[101] M. Bregant[114] M. Broz[38] G. E. Bruno[34a,34b,100] M. D. Buckland[26] D. Budnikov[146] H. Buesching[68] S. Bufalino[32] P. Buhler[106] N. Burmasov[146] Z. Buthelezi[72,127] A. Bylinkin[21] S. A. Bysiak,[111] M. Cai[6] H. Caines[142] A. Caliva[31] E. Calvo Villar[105] J. M. M. Camacho[113] P. Camerini[26] F. D. M. Canedo[114] S. L. Cantway[142] M. Carabas[117] A. A. Carballo[35] F. Carnesecchi[35] R. Caron[132] L. A. D. Carvalho[114] J. Castillo Castellanos[134] F. Catalano[27,35] C. Ceballos Sanchez[147] I. Chakaberia[78] P. Chakraborty[50] S. Chandra[139] S. Chapeland[35] M. Chartier[123] S. Chattopadhyay[139] S. Chattopadhyay[103] T. Cheng[6,101] C. Cheshkov[132] B. Cheynis[132] V. Chibante Barroso[35] D. D. Chinellato[115] E. S. Chizzali[99,‡] J. Cho[62] S. Cho[62] P. Chochula[35] D. Choudhury,[44] P. Christakoglou[88] C. H. Christensen[87] P. Christiansen[79] T. Chujo[129] M. Ciacco[32] C. Cicalo[55] F. Cindolo[54] M. R. Ciupek,[101] G. Clai,[54,§] F. Colamaria[53] J. S. Colburn,[104] D. Colella[34a,34b,100] M. Colocci[28] M. Concas[35] G. Conesa Balbastre[77] Z. Conesa del Valle[135] G. Contin[26] J. G. Contreras[38] M. L. Coquet[134] P. Cortese[60,137] M. R. Cosentino[116] F. Costa[35] S. Costanza[23,58] C. Cot[135] J. Crkovská[98] P. Crochet[131] R. Cruz-Torres[78] P. Cui[6] A. Dainese[57] M. C. Danisch[98] A. Danu[67] P. Das[84] P. Das[4a,4b] S. Das[4a,4b] A. R. Dash[130] S. Dash[50] A. De Caro[31] G. de Cataldo[53] J. de Cuveland,[41] A. De Falco[24] D. De Gruttola[31] N. De Marco[60] C. De Martin[26] S. De Pasquale[31] R. Deb[138] R. Del Grande[99] L. Dello Stritto[31] W. Deng[6] P. Dhankher[19] D. Di Bari[34a,34b] A. Di Mauro[35] B. Diab[134] R. A. Diaz[7,147] T. Dietel[118] Y. Ding[6] J. Ditzel[68] R. Divià[19] D. U. Dixit[19] Ø. Djuvsland,[21] U. Dmitrieva[146] A. Dobrin[67] B. Dönigus[68] J. M. Dubinski[140] A. Dubla[101] S. Dudi[94] P. Dupieux[131] M. Durkac,[110] N. Dzalaiova,[13] T. M. Eder[130] R. J. Ehlers[78] F. Eisenhut[68] R. Ejima[96] D. Elia[53] B. Erazmus[107] F. Ercolessi[28] B. Espagnon[135] G. Eulisse[35] D. Evans[104] S. Evdokimov[146] L. Fabbietti[99] M. Faggin[30] J. Faivre[77] F. Fan[6] W. Fan[78] A. Fantoni[52] M. Fasel[91] P. Fecchio[32] A. Feliciello[60] G. Feofilov[146] A. Fernández Téllez[47] L. Ferrandi[114] M. B. Ferrer[35] A. Ferrero[134] C. Ferrero[60,‖] A. Ferretti[27] V. J. G. Feuillard[98] V. Filova[38] D. Finogeev[146] F. M. Fionda[55] F. Flor[120] A. N. Flores[112] S. Foertsch[72] I. Fokin[98] S. Fokin[146] E. Fragiacomo[61] E. Frajna[49] U. Fuchs[35] N. Funicello[31] C. Furget[77] A. Furs[146] T. Fusayasu[102] J. J. Gaardhøje[87] M. Gagliardi[27] A. M. Gago[105] T. Gahlaut[50] C. D. Galvan[113] D. R. Gangadharan[120] P. Ganoti[82] C. Garabatos[101] T. García Chávez[47] E. Garcia-Solis[9] C. Gargiulo[35] P. Gasik[101] A. Gautam[122] M. B. Gay Ducati[70] M. Germain[107] A. Ghimouz[129] C. Ghosh,[139] M. Giacalone[54] G. Gioachin[32] P. Giubellino[60,101] P. Giubilato[30] A. M. C. Glaenzer[134] P. Glässel[98] E. Glimos[126] D. J. Q. Goh[80] V. Gonzalez[141] M. Gorgon[2] K. Goswami[51] S. Gotovac,[36] V. Grabski[71] L. K. Graczykowski[140] E. Grecka[90] A. Grelli[63] C. Grigoras[35] V. Grigoriev[146] S. Grigoryan[1,147] F. Grosa[35] J. F. Grosse-Oetringhaus[35] R. Grosso[101] D. Grund[38] N. A. Grunwald,[98] G. G. Guardiano[115] R. Guernane[77] M. Guilbaud[107] K. Gulbrandsen[87] T. Gündem[68] T. Gunji[128] W. Guo[6] A. Gupta[95] R. Gupta[95] R. Gupta[51] K. Gwizdziel[140] L. Gyulai[49] C. Hadjidakis[135] F. U. Haider[95] S. Haidlova[38] H. Hamagaki[80] A. Hamdi[78] Y. Han[143] B. G. Hanley[141] R. Hannigan[112] J. Hansen[79] M. R. Haque[140] J. W. Harris[142] A. Harton[9] H. Hassan[121] D. Hatzifotiadou[54] P. Hauer[45] L. B. Havener[142] S. T. Heckel[99] E. Hellbär[101] H. Helstrup[37] M. Hemmer[68] T. Herman[38] G. Herrera Corral[8] F. Herrmann,[130] S. Herrmann[132] K. F. Hetland[37] B. Heybeck[68] H. Hillemanns[35] B. Hippolyte[133] F. W. Hoffmann[74] B. Hofman[63] G. H. Hong[143] M. Horst[99] A. Horzyk[2] Y. Hou[6] P. Hristov[35] C. Hughes[126] P. Huhn,[68] L. M. Huhta[121] T. J. Humanic[92] A. Hutson[120] D. Hutter[41] R. Ilkaev,[146] H. Ilyas[14] M. Inaba[129] G. M. Innocenti[35] M. Ippolitov[146] A. Isakov[88,90] T. Isidori[122] M. S. Islam[103] M. Ivanov,[13] M. Ivanov[101] V. Ivanov[146] K. E. Iversen[79] M. Jablonski[2] B. Jacak[78] N. Jacazio[28] P. M. Jacobs[78] S. Jadlovska[110] J. Jadlovsky[110] S. Jaelani[86] C. Jahnke[115] M. J. Jakubowska[140]

M. A. Janik [140] T. Janson,[74] S. Ji [17] S. Jia [10] A. A. P. Jimenez [69] F. Jonas [91,130] D. M. Jones [123] J. M. Jowett [35,101] J. Jung [68] M. Jung [68] A. Junique [35] A. Jusko [104] J. Kaewjai,[109] P. Kalinak [64] A. S. Kalteyer,[101] A. Kalweit [35] V. Kaplin [146] A. Karasu Uysal [76,¶] D. Karatovic [93] O. Karavichev [146] T. Karavicheva [146] P. Karczmarczyk [140] E. Karpechev [146] M. J. Karwowska [35,140] U. Kebschull [74] R. Keidel [145] D. L. D. Keijdener,[63] M. Keil [35] B. Ketzer,[45] S. S. Khade [51] A. M. Khan,[6,124] S. Khan [16] A. Khanzadeev [146] Y. Kharlov [146] A. Khatun [122] A. Khuntia [38] A. Kievsky [59] B. Kileng [37] B. Kim [108] C. Kim [17] D. J. Kim [121] E. J. Kim [73] J. Kim [143] J. S. Kim [43] J. Kim [62] J. Kim [73] M. Kim [19] S. Kim [18] T. Kim [143] K. Kimura [96] S. Kirsch [68] I. Kisel [41] S. Kiselev [146] A. Kisiel [140] J. P. Kitowski [2] J. L. Klay [5] J. Klein [35] S. Klein [78] C. Klein-Bösing [130] M. Kleiner [68] T. Klemenz [99] A. Kluge [35] A. G. Knospe [120] C. Kobdaj [109] T. Kollegger,[101] A. Kondratyev [147] N. Kondratyeva [146] E. Kondratyuk [146] J. Konig [68] S. König [22] S. A. Konigstorfer [99] P. J. Konopka [35] G. Kornakov [140] M. Korwieser [99] S. D. Koryciak [2] A. Kotliarov [90] V. Kovalenko [146] M. Kowalski [111] V. Kozhuharov [39] I. Králik [64] A. Kravčáková [40] L. Krcal [35,41] M. Krivda [64,104] F. Krizek [90] K. Krizkova Gajdosova [35] M. Kroesen [98] M. Krüger [68] D. M. Krupova [38] E. Kryshen [146] V. Kučera [62] C. Kuhn [133] P. G. Kuijer [88] T. Kumaoka,[129] D. Kumar,[139] L. Kumar [94] N. Kumar,[94] S. Kumar [34a,34b] S. Kundu [35] P. Kurashvili [83] A. Kurepin [146] A. B. Kurepin [146] A. Kuryakin [146] S. Kushpil [90] M. J. Kweon [62] Y. Kwon [143] S. L. La Pointe [41] P. La Rocca [29] A. Lakrathok,[109] M. Lamanna [35] A. R. Landou [77,119] R. Langoy [125] P. Larionov [35] E. Laudi [35] L. Lautner [35,99] R. Lavicka [106] R. Lea [58,138] H. Lee [108] I. Legrand [48] G. Legras [130] J. Lehrbach [41] T. M. Lelek,[2] R. C. Lemmon [89] I. León Monzón [113] M. M. Lesch [99] E. D. Lesser [19] P. Lévai [49] X. Li,[10] J. Lien [125] R. Lietava [104] I. Likmeta [120] B. Lim [27] S. H. Lim [17] V. Lindenstruth,[41] A. Lindner,[48] C. Lippmann [101] D. H. Liu,[6] J. Liu [123] G. S. S. Liveraro [115] I. M. Lofnes [21] C. Loizides [91] S. Lokos [111] J. Lömker [63] P. Loncar [36] X. Lopez [131] E. López Torres [7] P. Lu [101,124] F. V. Lugo [71] J. R. Luhder [130] M. Lunardon [30] G. Luparello [61] Y. G. Ma [42] M. Mager [35] A. Maire [133] E. M. Majerz,[2] M. V. Makariev [39] M. Malaev [146] G. Malfattore [28] N. M. Malik [95] Q. W. Malik,[20] S. K. Malik [95] L. Malinina [147,†,**] D. Mallick [84,135] N. Mallick [51] G. Mandaglio [33,56] S. K. Mandal [83] V. Manko [146] F. Manso [131] V. Manzari [53] Y. Mao [6] R. W. Marcjan [2] L. E. Marcucci [25] G. V. Margagliotti [26] A. Margotti [54] A. Marín [101] C. Markert [112] P. Martinengo [35] M. I. Martínez [47] G. Martínez García [107] M. P. P. Martins [114] S. Masciocchi [101] M. Masera [27] A. Masoni [55] L. Massacrier [135] O. Massen [63] A. Mastroserio [53,136] O. Matonoha [79] S. Mattiazzo [30] A. Matyja [111] C. Mayer [111] A. L. Mazuecos [35] F. Mazzaschi [27] M. Mazzilli [35] J. E. Mdhluli [127] Y. Melikyan [46] A. Menchaca-Rocha [71] J. E. M. Mendez [69] E. Meninno [106] A. S. Menon [120] M. Meres [13] S. Mhlanga,[72,118] Y. Miake,[129] L. Micheletti [35] D. L. Mihaylov [99] K. Mikhaylov [146,147] A. N. Mishra [49] D. Miśkowiec [101] A. Modak [4a,4b] B. Mohanty,[84] M. Mohisin Khan,[16,††] M. A. Molander [46] S. Monira [140] C. Mordasini,[121] D. A. Moreira De Godoy [130] I. Morozov [146] A. Morsch [35] T. Mrnjavac [35] V. Muccifora [52] S. Muhuri [139] J. D. Mulligan [78] A. Mulliri [24] M. G. Munhoz [114] R. H. Munzer [68] H. Murakami [128] S. Murray [118] L. Musa [35] J. Musinsky [64] J. W. Myrcha [140] B. Naik [127] A. I. Nambrath [19] B. K. Nandi [50] R. Nania [54] E. Nappi [53] A. F. Nassirpour [18] A. Nath [98] C. Nattrass [126] M. N. Naydenov [39] A. Neagu,[20] A. Negru,[117] L. Nellen [69] R. Nepeivoda [79] S. Nese [20] G. Neskovic [41] N. Nicassio [53] B. S. Nielsen [87] E. G. Nielsen [87] S. Nikolaev [146] S. Nikulin [146] V. Nikulin [146] F. Noferini [54] S. Noh [12] P. Nomokonov [147] J. Norman [123] N. Novitzky [91] P. Nowakowski [140] A. Nyanin [146] J. Nystrand [21] M. Ogino [80] S. Oh [18] A. Ohlson [79] A. Ohnishi [144] V. A. Okorokov [146] J. Oleniacz [140] A. C. Oliveira Da Silva [126] A. Onnerstad [121] C. Oppedisano [60] A. Ortiz Velasquez [69] J. Otwinowski [111] M. Oya,[96] K. Oyama [80] Y. Pachmayer [98] S. Padhan [50] D. Pagano [58,138] G. Paić [69] S. Paisano-Guzmán [47] A. Palasciano [53] S. Panebianco [134] H. Park [129] H. Park [108] J. Park [62] J. E. Parkkila [35] Y. Patley [50] R. N. Patra [95] B. Paul [24] H. Pei [6] T. Peitzmann [63] X. Peng [11] M. Pennisi [27] S. Perciballi [27] D. Peresunko [146] G. M. Perez [7] Y. Pestov,[146] V. Petrov [146] M. Petrovici [48] R. P. Pezzi [70,107] S. Piano [61] M. Pikna [13] P. Pillot [107] O. Pinazza [35,54] L. Pinsky,[120] C. Pinto [99] S. Pisano [52] M. Płoskoń [78] M. Planinic [93] F. Pliquett,[68] M. G. Poghosyan [91] B. Polichtchouk [146] S. Politano [32] N. Poljak [93] A. Pop [48] S. Porteboeuf-Houssais [131] V. Pozdniakov [147] I. Y. Pozos [47] K. K. Pradhan [51] S. K. Prasad [4a,4b] S. Prasad [51] R. Preghenella [54] F. Prino [60] C. A. Pruneau [141] I. Pshenichnov [146] M. Puccio [35] S. Pucillo [27] Z. Pugelova,[110] S. Qiu [88] L. Quaglia [27] S. Ragoni [15] A. Rai [142] A. Rakotozafindrabe [134] L. Ramello [60,137] F. Rami [133] T. A. Rancien,[77] M. Rasa [29] S. S. Räsänen [46] R. Rath [54] M. P. Rauch [21] I. Ravasenga [88] K. F. Read [91,126]

C. Reckziegel[116] A. R. Redelbach[41] K. Redlich[83,‡‡] C. A. Reetz[101] H. D. Regules-Medel,[47] A. Rehman,[21] F. Reidt[35] H. A. Reme-Ness[37] Z. Rescakova,[40] K. Reygers[98] A. Riabov[146] V. Riabov[146] R. Ricci[31] M. Richter[20] A. A. Riedel[99] W. Riegler[35] A. G. Riffero[27] C. Ristea[67] M. V. Rodriguez[35] M. Rodríguez Cahuantzi[47] S. A. Rodríguez Ramírez[47] K. Røed[20] R. Rogalev[146] E. Rogochaya[147] T. S. Rogoschinski[68] D. Rohr[35] D. Röhrich[21] P. F. Rojas,[47] S. Rojas Torres[38] P. S. Rokita[140] G. Romanenko[28] F. Ronchetti[52] A. Rosano[33,56] E. D. Rosas,[69] K. Roslon[140] A. Rossi[57] A. Roy[51] S. Roy[50] N. Rubini[28] D. Ruggiano[140] R. Rui[26] P. G. Russek[2] R. Russo[88] A. Rustamov[85] E. Ryabinkin[146] Y. Ryabov[146] A. Rybicki[111] H. Rytkonen[121] J. Ryu[17] W. Rzesa[140] O. A. M. Saarimaki[46] S. Sadhu,[34a,34b] S. Sadovsky[146] J. Saetre[21] K. Šafařík[38] P. Saha,[44] S. K. Saha[4a,4b] S. Saha[84] B. Sahoo[50] B. Sahoo[51] R. Sahoo[51] S. Sahoo,[65] D. Sahu[51] P. K. Sahu[65] J. Saini[139] K. Sajdakova,[40] S. Sakai[129] M. P. Salvan[101] S. Sambyal[95] D. Samitz[106] I. Sanna[35,99] T. B. Saramela,[114] P. Sarma[44] V. Sarritzu[24] V. M. Sarti[99] M. H. P. Sas[142] S. Sawan[84] J. Schambach[91] H. S. Scheid[68] C. Schiaua[48] R. Schicker[98] A. Schmah,[101] C. Schmidt[101] H. R. Schmidt,[97] M. O. Schmidt[35] M. Schmidt,[97] N. V. Schmidt[91] A. R. Schmier[126] R. Schotter[133] A. Schröter[41] J. Schukraft[35] K. Schweda[101] G. Scioli[28] E. Scomparin[60] J. E. Seger[15] Y. Sekiguchi,[128] D. Sekihata[128] M. Selina[88] I. Selyuzhenkov[101] S. Senyukov[133] J. J. Seo[62,98] D. Serebryakov[146] L. Šerkšnytė[99] A. Sevcenco,[67] T. J. Shaba[72] A. Shabetai[107] R. Shahoyan,[35] A. Shangaraev[146] A. Sharma,[94] B. Sharma[95] D. Sharma[50] H. Sharma[57,111] M. Sharma[95] S. Sharma[80] S. Sharma[95] U. Sharma[95] A. Shatat[135] O. Sheibani,[120] K. Shigaki[96] M. Shimomura,[81] J. Shin,[12] S. Shirinkin[146] Q. Shou[42] Y. Sibiriak[146] S. Siddhanta[55] T. Siemiarczuk[83] T. F. Silva[114] D. Silvermyr[79] T. Simantathammakul,[109] R. Simeonov[39] B. Singh,[95] B. Singh[99] K. Singh[51] R. Singh[84] R. Singh[95] R. Singh[51] S. Singh[16] V. K. Singh[139] V. Singhal[139] T. Sinha[103] B. Sitar[13] M. Sitta[60,137] T. B. Skaali[20] G. Skorodumovs[98] M. Slupecki[46] N. Smirnov[142] R. J. M. Snellings[63] E. H. Solheim[20] J. Song[17] C. Sonnabend[35,101] F. Soramel[30] A. B. Soto-hernandez[92] R. Spijkers[88] I. Sputowska[111] J. Staa[79] J. Stachel[98] I. Stan[67] P. J. Steffanic[126] S. F. Stiefelmaier[98] D. Stocco[107] I. Storehaug[20] P. Stratmann[130] S. Strazzi[28] A. Sturniolo,[33,56] C. P. Stylianidis,[88] A. A. P. Suaide[114] C. Suire[135] M. Sukhanov[146] M. Suljic[35] R. Sultanov[146] V. Sumberia[95] S. Sumowidagdo[86] S. Swain,[65] I. Szarka[13] M. Szymkowski[140] S. F. Taghavi[99] G. Taillepied[101] J. Takahashi[115] G. J. Tambave[84] S. Tang[6] Z. Tang[124] J. D. Tapia Takaki[122] N. Tapus,[117] L. A. Tarasovicova,[130] M. G. Tarzila[48] G. F. Tassielli[34a,34b] A. Tauro[35] A. Tavira García[135] G. Tejeda Muñoz[47] A. Telesca[35] L. Terlizzi[27] C. Terrevoli[120] S. Thakur[4a,4b] D. Thomas,[112] A. Tikhonov[146] A. R. Timmins[120] M. Tkacik[110] T. Tkacik[110] A. Toia[68] R. Tokumoto,[96] K. Tomohiro,[96] N. Topilskaya[146] M. Toppi[52] T. Tork[135] V. V. Torres[107] A. G. Torres Ramos[34a,34b] A. Trifiró[33,56] A. S. Triolo[33,35,56] S. Tripathy[54] T. Tripathy[50] S. Trogolo[35] V. Trubnikov[3] W. H. Trzaska[121] T. P. Trzcinski[140] A. Tumkin[146] R. Turrisi[57] T. S. Tveter[20] K. Ullaland[21] B. Ulukutlu[99] A. Uras[132] G. L. Usai[24] M. Vala,[40] N. Valle[23] L. V. R. van Doremalen[63] M. van Leeuwen[88] C. A. van Veen[98] R. J. G. van Weelden[88] P. Vande Vyvre[35] D. Varga[49] Z. Varga[49] M. Vasileiou[82] A. Vasiliev[146] O. Vázquez Doce[52] O. Vazquez Rueda[120] V. Vechernin[146] E. Vercellin[27] S. Vergara Limón,[47] R. Verma,[50] L. Vermunt[101] R. Vértesi[49] M. Verweij[63] L. Vickovic,[36] Z. Vilakazi,[127] O. Villalobos Baillie[104] A. Villani[26] A. Vinogradov[146] T. Virgili[31] M. M. O. Virta[121] V. Vislavicius,[79] M. Viviani[59] A. Vodopyanov[147] B. Volkel[35] M. A. Völkl[98] K. Voloshin,[146] S. A. Voloshin[141] G. Volpe[34a,34b] B. von Haller[35] I. Vorobyev[99] N. Vozniuk[146] J. Vrláková[40] J. Wan,[42] C. Wang[42] D. Wang,[42] Y. Wang[42] Y. Wang[6] A. Wegrzynek[35] F. T. Weiglhofer,[41] S. C. Wenzel[35] J. P. Wessels[130] J. Wiechula[68] J. Wikne[20] G. Wilk[83] J. Wilkinson[101] G. A. Willems[130] B. Windelband[98] M. Winn[134] J. R. Wright[112] W. Wu,[42] Y. Wu[124] R. Xu[6] A. Yadav[45] A. K. Yadav[139] S. Yalcin[76] Y. Yamaguchi[96] S. Yang,[21] S. Yano[96] Z. Yin[6] I.-K. Yoo[17] J. H. Yoon[62] H. Yu,[12] S. Yuan,[21] A. Yuncu[98] V. Zaccolo[26] C. Zampolli[35] F. Zanone[98] N. Zardoshti[35] A. Zarochentsev[146] P. Závada[66] N. Zaviyalov,[146] M. Zhalov[146] B. Zhang[6] C. Zhang[134] L. Zhang[42] S. Zhang[42] X. Zhang[6] Y. Zhang,[124] Z. Zhang[6] M. Zhao[10] V. Zherebchevskii,[146] Y. Zhi[10] D. Zhou[6] Y. Zhou[87] J. Zhu[6,57] Y. Zhu[6] S. C. Zugravel[60] and N. Zurlo[58,138]

(ALICE Collaboration)

[1]A.I. Alikhanyan National Science Laboratory (Yerevan Physics Institute) Foundation, Yerevan, Armenia
[2]AGH University of Krakow, Cracow, Poland
[3]Bogolyubov Institute for Theoretical Physics, National Academy of Sciences of Ukraine, Kiev, Ukraine
[4a]Bose Institute, Department of Physics, Kolkata, India
[4b]Centre for Astroparticle Physics and Space Science (CAPSS), Kolkata, India
[5]California Polytechnic State University, California, USA
[6]Central China Normal University, Wuhan, China
[7]Centro de Aplicaciones Tecnológicas y Desarrollo Nuclear (CEADEN), Havana, Cuba
[8]Centro de Investigación y de Estudios Avanzados (CINVESTAV), Mexico City and Mérida, Mexico
[9]Chicago State University, Chicago, Illinois, USA
[10]China Institute of Atomic Energy, Beijing, China
[11]China University of Geosciences, Wuhan, China
[12]Chungbuk National University, Cheongju, Republic of Korea
[13]Comenius University Bratislava, Faculty of Mathematics, Physics and Informatics,
Bratislava, Slovak Republic
[14]COMSATS University Islamabad, Islamabad, Pakistan
[15]Creighton University, Nebraska, USA
[16]Department of Physics, Aligarh Muslim University, Aligarh, India
[17]Department of Physics, Pusan National University, Pusan, Republic of Korea
[18]Department of Physics, Sejong University, Seoul, Republic of Korea
[19]Department of Physics, University of California, Berkeley, California, USA
[20]Department of Physics, University of Oslo, Oslo, Norway
[21]Department of Physics and Technology, University of Bergen, Bergen, Norway
[22]Department of Physics, North Carolina State University, Raleigh, North Carolina, USA
[23]Dipartimento di Fisica, Università di Pavia, Pavia, Italy
[24]Dipartimento di Fisica dell'Università, Cagliari, Italy and Sezione INFN, Cagliari, Italy
[25]Dipartimento di Fisica dell'Università, Pisa, Italy and Sezione INFN, Pisa, Italy
[26]Dipartimento di Fisica dell'Università, Trieste, Italy and Sezione INFN, Trieste, Italy
[27]Dipartimento di Fisica dell'Università, Turin, Italy and Sezione INFN, Turin, Italy
[28]Dipartimento di Fisica e Astronomia dell'Università, Bologna, Italy and Sezione INFN, Bologna, Italy
[29]Dipartimento di Fisica e Astronomia dell'Università, Catania, Italy and Sezione INFN, Catania, Italy
[30]Dipartimento di Fisica e Astronomia dell'Università, Padova, Italy and Sezione INFN, Padova, Italy
[31]Dipartimento di Fisica 'E.R. Caianiello' dell'Università, Salerno, Italy and Gruppo Collegato INFN,
Salerno, Italy
[32]Dipartimento DISAT del Politecnico and Sezione INFN, Turin, Italy
[33]Dipartimento di Scienze MIFT, Università di Messina, Messina, Italy
[34a]Dipartimento Interateneo di Fisica 'M. Merlin', Bari, Italy
[34b]Sezione INFN, Bari, Italy
[35]European Organization for Nuclear Research (CERN), Geneva, Switzerland
[36]Faculty of Electrical Engineering, Mechanical Engineering and Naval Architecture,
University of Split, Split, Croatia
[37]Faculty of Engineering and Science, Western Norway University of Applied Sciences, Bergen, Norway
[38]Faculty of Nuclear Sciences and Physical Engineering, Czech Technical University in Prague,
Prague, Czech Republic
[39]Faculty of Physics, Sofia University, Sofia, Bulgaria
[40]Faculty of Science, P.J. Šafárik University, Košice, Slovak Republic
[41]Frankfurt Institute for Advanced Studies, Johann Wolfgang Goethe-Universität Frankfurt,
Frankfurt, Germany
[42]Fudan University, Shanghai, China
[43]Gangneung-Wonju National University, Gangneung, Republic of Korea
[44]Gauhati University, Department of Physics, Guwahati, India
[45]Helmholtz-Institut für Strahlen- und Kernphysik,
Rheinische Friedrich-Wilhelms-Universität Bonn, Bonn, Germany
[46]Helsinki Institute of Physics (HIP), Helsinki, Finland
[47]High Energy Physics Group, Universidad Autónoma de Puebla, Puebla, Mexico
[48]Horia Hulubei National Institute of Physics and Nuclear Engineering, Bucharest, Romania
[49]HUN-REN Wigner Research Centre for Physics, Budapest, Hungary
[50]Indian Institute of Technology Bombay (IIT), Mumbai, India
[51]Indian Institute of Technology Indore, Indore, India

[52]*INFN, Laboratori Nazionali di Frascati, Frascati, Italy*
[53]*INFN, Sezione di Bari, Bari, Italy*
[54]*INFN, Sezione di Bologna, Bologna, Italy*
[55]*INFN, Sezione di Cagliari, Cagliari, Italy*
[56]*INFN, Sezione di Catania, Catania, Italy*
[57]*INFN, Sezione di Padova, Padova, Italy*
[58]*INFN, Sezione di Pavia, Pavia, Italy*
[59]*INFN, Sezione di Pisa, Pisa, Italy*
[60]*INFN, Sezione di Torino, Turin, Italy*
[61]*INFN, Sezione di Trieste, Trieste, Italy*
[62]*Inha University, Incheon, Republic of Korea*
[63]*Institute for Gravitational and Subatomic Physics (GRASP),
Utrecht University/Nikhef, Utrecht, Netherlands*
[64]*Institute of Experimental Physics, Slovak Academy of Sciences, Slovak Republic*
[65]*Institute of Physics, Homi Bhabha National Institute, Bhubaneswar, India*
[66]*Institute of Physics of the Czech Academy of Sciences, Prague, Czech Republic*
[67]*Institute of Space Science (ISS), Bucharest, Romania*
[68]*Institut für Kernphysik, Johann Wolfgang Goethe-Universität Frankfurt, Frankfurt, Germany*
[69]*Instituto de Ciencias Nucleares, Universidad Nacional Autónoma de México, Mexico City, Mexico*
[70]*Instituto de Física, Universidade Federal do Rio Grande do Sul (UFRGS), Porto Alegre, Brazil*
[71]*Instituto de Física, Universidad Nacional Autónoma de México, Mexico City, Mexico*
[72]*iThemba LABS, National Research Foundation, Somerset West, South Africa*
[73]*Jeonbuk National University, Jeonju, Republic of Korea*
[74]*Johann-Wolfgang-Goethe Universität Frankfurt Institut für Informatik,
Fachbereich Informatik und Mathematik, Frankfurt, Germany*
[75]*Korea Institute of Science and Technology Information, Daejeon, Republic of Korea*
[76]*KTO Karatay University, Konya, Turkey*
[77]*Laboratoire de Physique Subatomique et de Cosmologie, Université Grenoble-Alpes, CNRS-IN2P3,
Grenoble, France*
[78]*Lawrence Berkeley National Laboratory, Berkeley, California, USA*
[79]*Lund University Department of Physics, Division of Particle Physics, Lund, Sweden*
[80]*Nagasaki Institute of Applied Science, Nagasaki, Japan*
[81]*Nara Women's University (NWU), Nara, Japan*
[82]*National and Kapodistrian University of Athens,
School of Science, Department of Physics, Athens, Greece*
[83]*National Centre for Nuclear Research, Warsaw, Poland*
[84]*National Institute of Science Education and Research, Homi Bhabha National Institute, Jatni, India*
[85]*National Nuclear Research Center, Baku, Azerbaijan, Baku, Azerbaijan*
[86]*National Research and Innovation Agency-BRIN, Jakarta, Indonesia*
[87]*Niels Bohr Institute, University of Copenhagen, Copenhagen, Denmark*
[88]*Nikhef, National institute for subatomic physics, Amsterdam, Netherlands*
[89]*Nuclear Physics Group, STFC Daresbury Laboratory, Daresbury, United Kingdom*
[90]*Nuclear Physics Institute of the Czech Academy of Sciences, Husinec-Řež, Czech Republic*
[91]*Oak Ridge National Laboratory, Oak Ridge, Tennessee, USA*
[92]*Ohio State University, Columbus, Ohio, USA*
[93]*Physics department, Faculty of science, University of Zagreb, Zagreb, Croatia*
[94]*Physics Department, Panjab University, Chandigarh, India*
[95]*Physics Department, University of Jammu, Jammu, India*
[96]*Physics Program and International Institute for Sustainability with Knotted Chiral Meta Matter
(SKCM2), Hiroshima University, Hiroshima, Japan*
[97]*Physikalisches Institut, Eberhard-Karls-Universität Tübingen, Tübingen, Germany*
[98]*Physikalisches Institut, Ruprecht-Karls-Universität Heidelberg, Heidelberg, Germany*
[99]*Physik Department, Technische Universität München, Munich, Germany*
[100]*Politecnico di Bari, Bari, Italy*
[101]*Research Division and ExtreMe Matter Institute EMMI,
GSI Helmholtzzentrum für Schwerionenforschung GmbH, Darmstadt, Germany*
[102]*Saga University, Saga, Japan*
[103]*Saha Institute of Nuclear Physics, Homi Bhabha National Institute, Kolkata, India*
[104]*School of Physics and Astronomy, University of Birmingham, Birmingham, United Kingdom*
[105]*Sección Física, Departamento de Ciencias, Pontificia Universidad Católica del Perú, Lima, Peru*

[106]Stefan Meyer Institut für Subatomare Physik (SMI), Vienna, Austria

[107]SUBATECH, IMT Atlantique, Nantes Université, CNRS-IN2P3, Nantes, France

[108]Sungkyunkwan University, Suwon City, Republic of Korea

[109]Suranaree University of Technology, Nakhon Ratchasima, Thailand

[110]Technical University of Košice, Košice, Slovak Republic

[111]The Henryk Niewodniczanski Institute of Nuclear Physics, Polish Academy of Sciences, Cracow, Poland

[112]The University of Texas at Austin, Austin, Texas, USA

[113]Universidad Autónoma de Sinaloa, Culiacán, Mexico

[114]Universidade de São Paulo (USP), São Paulo, Brazil

[115]Universidade Estadual de Campinas (UNICAMP), Campinas, Brazil

[116]Universidade Federal do ABC, Santo Andre, Brazil

[117]Universitatea Nationala de Stiinta si Tehnologie Politehnica Bucuresti, Bucharest, Romania

[118]University of Cape Town, Cape Town, South Africa

[119]University of Derby, Derby, United Kingdom

[120]University of Houston, Houston, Texas, USA

[121]University of Jyväskylä, Jyväskylä, Finland

[122]University of Kansas, Lawrence, Kansas, USA

[123]University of Liverpool, Liverpool, United Kingdom

[124]University of Science and Technology of China, Hefei, China

[125]University of South-Eastern Norway, Kongsberg, Norway

[126]University of Tennessee, Knoxville, Tennessee, USA

[127]University of the Witwatersrand, Johannesburg, South Africa

[128]University of Tokyo, Tokyo, Japan

[129]University of Tsukuba, Tsukuba, Japan

[130]Universität Münster, Institut für Kernphysik, Münster, Germany

[131]Université Clermont Auvergne, CNRS/IN2P3, LPC, Clermont-Ferrand, France

[132]Université de Lyon, CNRS/IN2P3, Institut de Physique des 2 Infinis de Lyon, Lyon, France

[133]Université de Strasbourg, CNRS, IPHC UMR 7178, F-67000 Strasbourg, France, Strasbourg, France

[134]Université Paris-Saclay, Centre d'Etudes de Saclay (CEA), IRFU, Départment de Physique Nucléaire (DPhN), Saclay, France

[135]Université Paris-Saclay, CNRS/IN2P3, IJCLab, Orsay, France

[136]Università degli Studi di Foggia, Foggia, Italy

[137]Università del Piemonte Orientale, Vercelli, Italy

[138]Università di Brescia, Brescia, Italy

[139]Variable Energy Cyclotron Centre, Homi Bhabha National Institute, Kolkata, India

[140]Warsaw University of Technology, Warsaw, Poland

[141]Wayne State University, Detroit, Michigan, USA

[142]Yale University, Connecticut, USA

[143]Yonsei University, Seoul, Republic of Korea

[144]Yukawa Institute for Theoretical Physics, Kyoto University, Kyoto, Japan

[145]Zentrum für Technologie und Transfer (ZTT), Worms, Germany

[146]Affiliated with an institute covered by a cooperation agreement with CERN

[147]Affiliated with an international laboratory covered by a cooperation agreement with CERN

[†]Deceased.

[‡]Also at Max-Planck-Institut fur Physik, Munich, Germany.

[§]Also at Italian National Agency for New Technologies, Energy and Sustainable Economic Development (ENEA), Bologna, Italy.

[‖]Also at Dipartimento DET del Politecnico di Torino, Turin, Italy.

[¶]Also at Yildiz Technical University, Istanbul, Türkiye.

[**]Also at An institution covered by a cooperation agreement with CERN.

[††]Also at Department of Applied Physics, Aligarh Muslim University, Aligarh, India.

[‡‡]Also at Institute of Theoretical Physics, University of Wroclaw, Poland.